Available online at www.sciencedirect.com
SCIENCE DIRECT®
Journal of Electrostatics 61 (2004) 85–98
Journal of ELECTROSTATICS
www.elsevier.com/locate/elstat

Simulation of corona discharge in point–plane configuration ☆

K. Adamiak[a,*], P. Atten[b]

[a] *Department of Electrical and Computer Engineering, University of Western Ontario, London, Ont., Canada N6A 5B9*
[b] *Laboratoire d'Electrostatique et de Matériaux Diélectriques, CNRS and Joseph Fourier University, Grenoble, France*

Received 28 June 2003; received in revised form 2 January 2004; accepted 25 January 2004

Abstract

A numerical technique is proposed for determining the distributions of electric field and charge density in the case of a positive corona discharge in gas in the point–plane geometry. This technique is based on the boundary and finite elements methods for obtaining the harmonic and space charge components of the electric field, respectively, and on the method of characteristics to determine the charge density distribution. The numerical simulation gives the current density distribution on the ground plate, which compares favorably with the ones measured using a cylinder–cone needle with a tip of spherical shape.

Keywords: Corona; Numerical simulation; Current density; Voltage current characteristic

1. Introduction

Despite widespread use of the electric corona discharge, there is no reliable and accurate numerical model for the computer simulation of this phenomenon. Existing numerical techniques are sufficient for rough estimate of the basic characteristics of the discharge ($V-I$ curve, electric field, current density), when the corona electrode

☆ Presented at the 2003 Joint Meeting of the Electrostatics Society of America and the IEEE Industry Applications Society Electrostatic Processes Committee, June 24–27, 2003, Little Rock, AR, USA.

*Corresponding author. Tel.: +1-519-6612111e88358; fax: +1-519-661-3488.
E-mail addresses: kadamiak@eng.uwo.ca (K. Adamiak), atten@labs.polycnrs-gre.fr (P. Atten).

0304-3886/$ - see front matter
doi:10.1016/j.elstat.2004.01.021

is not too sharp. However, they fail if high accuracy of results is required or in the case of electrodes with very small radii of curvature.

The main reason for the lack of a more sophisticated corona simulation algorithm is complexity of this phenomenon. The full model in two-dimensional space has been attempted by very few authors. Morrow [1] was the first who tried to analyze all essential processes (ionization, attachment of electrons, recombination, etc.) in the time domain. He was apparently successful, although the results were not validated experimentally, but the algorithm must have led to very time consuming computations due to a very fine spatial discretization needed, especially in the ionization layer, and very irregular dynamics of the problem, with rapid time variation of some parameters followed by much longer intervals of relatively slow changes. Therefore, such an approach can be useful for detailed study of some physical processes, but not as a design or optimization tool in engineering applications.

Much better documented are one-dimensional models, which do not require so demanding computer resources [2]. Pontiga and others have concentrated their interest on the numerous processes and chemical reactions occurring in the corona discharge [3]. However, this was done for steady-state conditions.

Nearly all the authors interested in engineering applications of the corona discharge completely ignore the processes in the ionization layer, what is justified by its small thickness, generally on the order of the corona electrode radius of curvature [4]. The ionization of gas is, by definition, limited to this layer, but attachment is not for the negative corona; nobody yet has tried to investigate these effects outside the ionization layer. The most common approach is to consider the two-dimensional DC monopolar model, where one species of ionic charges is injected from the discharge electrode and the ions trajectories are predicted by solving coupled equations for the electric field and the charge transport. Many versions of this basic monopolar corona model differ by using various numerical techniques. Iterative algorithms are predominant, where both problems are solved subsequently, until convergence is reached. A different philosophy has been presented only by Feng [5], who combined both equations into a one non-linear set of partial differential equations.

Differential techniques are preferred for the Poisson equation governing the electric field distribution. Earlier attempts with the finite difference method could not handle the sharp geometry of the discharge electrode very well [6]. The finite element method (FEM) has removed this limitation and is commonly accepted [7], although a proper discretization may lead to quite large algebraic systems. The boundary techniques (charge simulation method and boundary element method) are better suited to strong field gradients, but inclusion of the space charge is much troublesome [8].

Choice of the numerical technique for the charge transport equation is much less obvious. Three basic groups of methods can be identified:

- the method of characteristics (MOC), which predicts the space charge density along some lines, called characteristics, which are the field lines and ions trajectories here [9].

- the finite volume method, especially in the version called the donor-cell method, using the charge conservation equation in the integral form [10].
- the FEM, which may be prone to the numerical diffusion, predicting some space charge density in the whole space while in reality it is limited to some area between both electrodes [5].

Interfacing both problems (electric field and space charge) may be problematic in some combination of the techniques mentioned above. The differential techniques for the electric field require values of the space charge density at the model nodes, while the MOC calculates them at its own set of points. From the most common suggestions, one proposes to regenerate the mesh at each iteration step [11] and another one uses a special interpolation of charges [12]. Both can significantly extend the computing time.

This paper presents a hybrid approach to the monopolar corona modeling: the electric field is solved by combined BEM-FEM technique. The first one is used for the Laplace equation, and the second one for the Poisson equation. The MOC handles the charge transport equation and a simple interpolation scheme provides an interface between both steps. The Kaptzov assumption (restricted to the zone of the needle electrode where the corona discharge sustains) is approximately satisfied by introducing an injection law, which gives the density of injected charge carriers as a function of the local field. This leads to delineate the part of the needle where the corona discharge takes place and, hence, to determine the inter-electrode zone with non zero charge density. In particular the radius at which the current density on the ground plate abruptly decreases down to zero is well predicted for different values of the tip radius and the needle-plate distance.

A close examination of computed and measured current–voltage characteristics $I(V)$ shows that their shape is well predicted and that a good approximation is given by the expression $I = aK\varepsilon V(V - V_0)/d$ where K is the ions mobility, ε the gas permittivity, V the applied voltage and V_0 the corona onset level. The constant a takes a value close to 1.58. This makes it possible to estimate the mobility of ions from the $I(V)$ measurement.

2. Numerical model

A classical electric corona discharge configuration is investigated in this paper with two electrodes of distinctly different radii of curvature separated by some air gap. The sharp electrode is supplied with a positive high voltage and one species of positive ions is injected into air gap. These ions move with a constant mobility towards the grounded plate. As the space charge is present, the distribution of electric scalar potential V is governed by the Poisson equation

$$\varepsilon \nabla^2 V = -\rho, \tag{1}$$

where ρ is the space charge density. The density of the ionic current is defined as

$$\boldsymbol{J} = K\rho\boldsymbol{E}, \tag{2}$$

where $\boldsymbol{E} = -\nabla V$ is the electric field and it should satisfy the charge conservation law:

$$\nabla \cdot \boldsymbol{J} = 0. \tag{3}$$

Eq. (2) is valid for a stationary gas at uniform temperature when diffusion can be ignored [13], assumption which was used in the present numerical model. After some operations the following partial differential equation can be derived for the space charge density:

$$\nabla\rho \cdot \nabla V = \frac{\rho^2}{\varepsilon}. \tag{4}$$

Eqs. (1)—linear for the electric potential—and (4)—nonlinear for the space charge—form a set of two partial differential equations governing the problem.

Proper boundary conditions should be formulated for a complete description. The potential V satisfies the classical Dirichlet conditions with a known potential on the discharge electrode and zero potential on the ground plate. Strict boundary conditions for the charge density cannot be formulated as all essential ionization processes next to the corona electrode have been neglected; therefore some kind of injection law must be assumed. The gas molecules can be ionized, if the following ionization criterion is satisfied [14]:

$$\int \alpha_{\mathrm{T}}(r)\,\mathrm{d}r = \ln(1 + 1/\gamma), \tag{5}$$

where α_{T} is the Townsend ionization coefficient and γ is the Townsend coefficient of secondary electron emission. For air at normal conditions the ionization coefficient is given as [14]

$$\alpha_{\mathrm{T}}(E) = Ap[(E/E_0)^2 - 1] \quad \text{for } E \geqslant E_0, \tag{6}$$

where E_0 is a critical electric field and A is a constant.

One possible approach to this problem is to vary the magnitudes of charge injected from these points on the electrode where $E > E_0$, until condition (5) is satisfied [4]. This idea works fine, even though the computing time is relatively long as the numerical integration needed to estimate (5) has to be performed for many different points and for each iteration. The problem can be much simplified if an additional hypothesis, firstly suggested by Kaptzov, is accepted [15]. He suggested that if the corona discharge occurs at some point of the electrode and charge is injected, the electric field at this point remains at the value it takes at the corona onset.

Kaptzov's hypothesis can be used to create a simple algorithm, which helps to establish the charge injection law. The potential of the corona electrode should be increased step by step and condition (5) checked at each point of the electrode. When it is satisfied, the potential of the electrode defines the corona onset level at this point, and the corresponding value of the electric field will be the critical electric field at this point, which remains constant during the discharge. After such calculations have been completed, a critical electric field will be assigned to each point on the electrode, and can be used later in the corona simulation.

Two versions of the charge injection law were tested in [4]. The first one used the direct ionization criterion and did not rely on Kaptzov's assumption. The second one satisfied the ionization criterion at the onset level only and assumed that the electric field does not change when the corona is produced. Both have led to slightly different distributions of the space charge and electric field, especially on the corona electrode. Surprisingly, the global $V-I$ characteristics were practically the same when the electrode voltage was not too large.

For highly symmetrical arrangements of electrodes, for example one-dimensional cylindrical or spherical ones, there exists an analytical solution for the harmonic field. In these cases the critical electric field can be derived analytically from the ionization criterion (5). The result is known as Peek's equation and in air it has the following forms [16]:

- cylindrical geometry

$$E_0 = 3.1 \times 10^4 \delta \left(1 + \frac{0.308}{\sqrt{\delta r}}\right), \tag{7}$$

- spherical geometry

$$E_0 = 3.1 \times 10^4 \delta \left(1 + \frac{0.308}{\sqrt{0.5\delta r}}\right), \tag{8}$$

where

$$\delta = \frac{T_0 P}{T P_0}$$

and r is the electrode radius in cm, T_0 the standard temperature, T the actual temperature, P_0 the standard pressure and P the actual pressure of gas. It must be emphasized that these Peek's equations can be used only, if the electric field is the same at all points of the discharge electrodes.

3. Computational algorithm

A hybrid FEM-BEM-MOC technique has been used to solve (1) and (4) and to find the magnitude and distribution of the injected charge. All steps are performed in a sequence forming two iterative loops.

3.1. Boundary element method

One of the most difficult issues in the corona simulation is the very strong gradient of the electric field close to the corona electrode. When the domain techniques are used, a very fine discretization has to be used, which results in a very large number of nodes. The BEM requires discretization of the electrodes only which leads to substantially smaller number of nodes. The solution at any point of the domain is

then calculated by an additional integration, which is more expensive, but the solution is very smooth and accurate.

In the case of Laplace equation, the following integral equation can be written for the surface charge density on the electrode surface, $\sigma(Q)$ [17]:

$$\int_{\Gamma} \sigma(Q)G(P,Q)\,\mathrm{d}s = V_0, \tag{9}$$

where $G(P,Q)$ is the problem Green function, which depends on the geometry (cylindrical or spherical) and V_0 is the electrode voltage. Only the corona electrode surface needs to be discretized as the proper form of the Green function can handle the effect of ground plate.

Eq. (9) is a Fredholm integral equation of the first kind and can be most conveniently solved by the BEM. The electrode surface has to be discretized into some number of elements, with some number of nodes identified in each. This procedure converts (9) into an algebraic set of equations with nodal values of the surface charge density σ as unknowns. This set is full, but the number of unknowns is much smaller than for the domain techniques. In the case studied in this paper a linear interpolation of solution was used (two nodes in each element) and the total number of nodes was between 100 and 150.

The BEM was used for the Laplace equation and this was done only once, at the beginning of the algorithm. The BEM solution was then used to generate the triangular mesh for the FEM part; nodes were created by intersection of the field lines and equipotential lines. Both components of the electric field at each mesh node were also calculated at this stage and stored for future use.

3.2. Finite element method

As the electric field generated by space charge cannot be conveniently handled by the BEM, the FEM has been used for this part. The non-uniform boundary conditions were satisfied by the BEM and uniform (zero) boundary conditions were assumed for the FEM. The whole domain was discretized into some number of the first-order triangular elements—typically between 10 000 and 20 000. Their distribution was non-uniform with very fine discretization near the discharge electrode and much larger elements in other areas. Conventional FEM procedure leads to formulation of the algebraic system with nodal values of the potential as unknowns [18]. The electric field values are then calculated by simple differentiation.

3.3. Method of characteristics [19]

The ion diffusion is usually very small and neglecting it leads to a very good approximation. In this case the MOC can be used. Along a characteristic line (which is a field line) defined by

$$\frac{\mathrm{d}\boldsymbol{r}}{\mathrm{d}t} = K\boldsymbol{E}, \tag{10}$$

the charge density satisfies an ordinary differential equation [19, p.74]:

$$\frac{\mathrm{d}\rho}{\mathrm{d}t} = -K\rho^2/\varepsilon \tag{11}$$

with a simple analytical solution

$$\frac{1}{\rho} = \frac{1}{\rho_0} + \frac{Kt}{\varepsilon}. \tag{12}$$

The characteristic lines are traced from those points on the corona electrode surface where the electric field is larger than the critical field, as only at those points the electric charge is injected. The charge begins with an initial value of ρ_0 and decays along the characteristics. Non-zero values of the charge exist between the axis of the system and the separatrix (last trajectory for the ions), which completely eliminates the problem of numerical diffusion, a common nuisance in all differential techniques.

3.4. Charge interpolation

The space charge from the MOC is calculated at some points, which are not related to the FEM mesh, where they are needed. Therefore, some interpolation algorithm is necessary. A simple technique has been implemented in this paper, where all MOC points are connected to form a triangular mesh. This procedure is not very expensive as the mesh is much smaller than for the FEM part and it does not have to be optimized or renumbered. Then, for any FEM mesh node the charge density is interpolated by finding a proper MOC mesh element and applying the linear interpolating function.

3.5. Charge density on the surface of the corona wire

The values of the charge density should be selected in order to satisfy the ionization criterion and the Kaptzov condition. This is in some sense an inverse problem and may be ill-posed in the strict sense [20]. A practical manifestation of this issue can be a slightly different final distribution of the charge density depending on some other parameters of the iteration process.

The electrode tip has a spherical shape, but the electric field is not constant and slightly varies from one point of the surface to another. Formally speaking the corona onset voltage and critical electric field would have to be different at all points. However, for the simplification of the algorithm, a constant critical electric field has been assumed as calculated from Peek's formula (8) for the spherical electrode.

The initial density of the space charge has to be guessed, or taken from a previous solution at similar conditions. After the problem is solved the electric field on the electrode surface is compared with Peek's value and the electric charge updated. While some well-founded techniques are often advised the following simple formula proved to be very effective:

$$\rho_{\mathrm{new}} = \rho_{\mathrm{old}} + B(E - E_0), \tag{13}$$

where B is an experimentally found constant.

3.6. Iterative loops

The whole algorithm has been arranged into two iterative loops. For a given space charge density on the corona electrode surface, the problem is solved for the charge density and electric field in the whole space. Eqs. (1) and (4) are solved iteratively until convergence is reached for both electric field and space charge density.

In the outer iterative loop the charge density on the electrode surface is iterated. This step is needed in order to satisfy the Kaptzov hypothesis, that the electric field on the corona electrode surface at the voltages larger than the onset value remains constant at Peek's value. Formally, such a condition can be treated as the third boundary condition for the electric potential with no boundary condition for the space charge density. In order to avoid this difficulty, the charge density on the electrode surface is iterated until the electric field is sufficiently close to Peek's experimental value.

4. Results

4.1. Geometry of the problem

The presented algorithm has been applied to the point–plane configuration. The point electrode was a 5 cm long cylindrical wire of 1 mm in diameter with a conical ending of 1 cm length and capped with a hemispherical tip [21]. Two different needles were tested with an average radius of curvature equal to 95 and 35 μm. The needles were mounted perpendicularly to the aluminum plate of 25 cm × 25 cm at the distance of 2 cm and 3.1 cm. The high voltage supplied to the needle varied between the corona onset level and 12 kV. Total corona current between both electrodes and the distribution of the current density on the ground plate were measured.

4.2. 95 μm electrode at 3.1 cm distance

The numerically calculated corona onset level was equal to 5.1 kV, which is close to the experimentally measured value of 4.91 kV (Table 1). The difference between these values can be attributed to the irregularities of the corona electrode surface: microscopic sharp points can ignite the corona discharge at lower voltages than for ideally smooth surface. When the voltage is increased above the onset level the total corona current increases faster than linearly with the voltage (Fig. 1). Both curves agree very well if the ions mobility is 2.3×10^{-4}. The conventionally accepted mobility 2.2×10^{-4} [22] would yield a larger discrepancy.

The I/V curve is almost perfectly linear and again shows very good agreement between experimental and computational results (Fig. 2). From a simplified analysis of the similar configuration, Sigmond [23] derived an approximate expression for the

Table 1
Experimental and calculated corona onset values for different geometries

Geometry	Experimental (kV)	Calculated (kV)	Error (%)
$R = 95\ \mu m, d = 3.1$ cm	4.91	5.1	3.87
$R = 95\ \mu m, d = 2$ cm	4.37	4.9	12.13
$R = 35\ \mu m, d = 3.1$ cm	3.91	4.25	8.7
$R = 35\ \mu m, d = 2$ cm	3.46	4.06	17.34

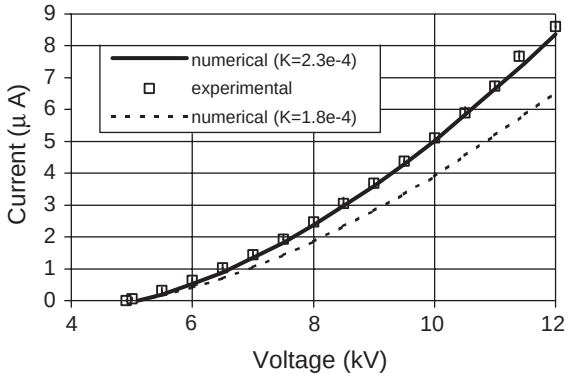

Fig. 1. Experimental and computational $V-I$ characteristics for the 95 μm needle 3.1 cm above the ground plate.

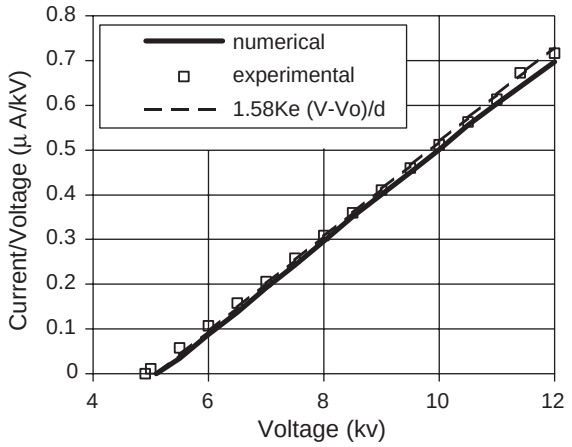

Fig. 2. I/V versus V characteristics for the point-plane configuration (95 μm needle, 3.1 cm above the ground plate).

$I-V$ characteristics:

$$I = aK\varepsilon V(V - V_0)/d, \tag{14}$$

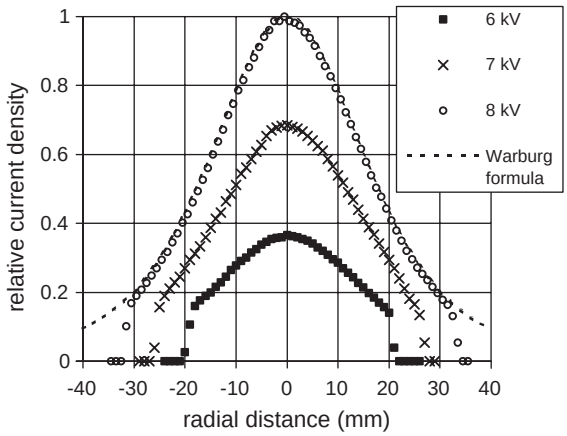

Fig. 3. Experimental distribution of the current density on the surface of ground plane. (95 μm needle 3.1 cm above the ground plate).

where $a \leqslant 2.0$. In our case the same formula would be valid if the parameter a is equal to 1.58. The experimental and computational data for the current density on the ground plate can be compared with the famous Warburg formula for the positive corona [23]:

$$J(\theta) = J(0)\cos^{4.82}\theta, \quad \theta \leqslant 60^\circ. \tag{15}$$

The measured densities of current on the ground plate for $V = 6, 7$ and 8 kV are shown in Fig. 3. All curves have been normalized with respect to the maximum current density at 8 kV. While there are some small differences, the experimental curves follow rather closely the Warburg curve. The current density abruptly decreases down to zero at some point, indicating that the ion diffusion has no significant effect. However, the point of abrupt decrease does not exactly follow the 60° angle as suggested by Warburg. The curves are not perfectly symmetrical probably due to defects of the needle tip.

The numerical curves (Fig. 4) preserve the same character, although the current decreases faster than measured experimentally, so the power of the Warburg cosine law would have to be different. Also, the point at which the current density decreases to zero is different from the measured one. For all curves there is a small minimum at the top of the curves. Such an effect was measured by some authors [24], but in this case is probably a numerical artifact.

4.3. Electrode with 95 μm tip at 2 cm

When the point–plane distance is reduced to 2 cm the general behavior of all results is similar. The experimental corona onset value of 4.37 kV is not far from 4.9 kV calculated numerically. The I/V versus V curve is still linear both for the experimental and computational data (Fig. 5). The curves are almost parallel first,

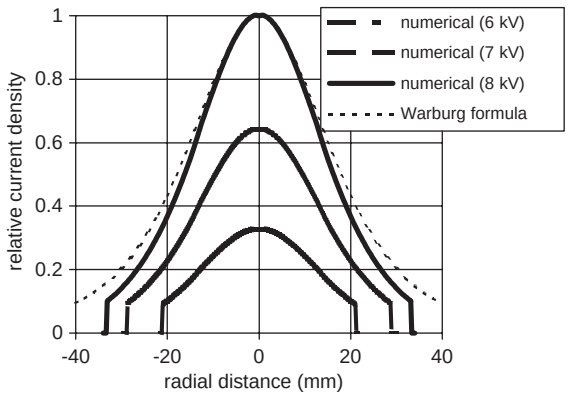

Fig. 4. Numerically calculated distributions of the current density on the ground plate for 6, 7 and 8 kV for the corona electrode with 95 μm radius of curvature.

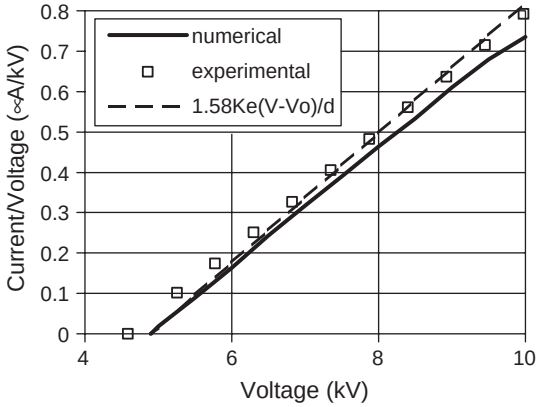

Fig. 5. I/V versus voltage characteristics for the 95 μm corona electrode at 2 cm from the ground plate.

with increasing distance at larger voltages. A simple theoretical formula can still be used to represent the curve, although its slope is slightly different now and the coefficient a would have to be adjusted for better match.

Experimental current density follows the Warburg formula very closely (Fig. 6), although again the curve abruptly changes to zero before 60° point.

4.4. Electrode with 35 μm tip

Agreement between experimental and computational data for the sharp corona electrode is not so good. At 3.1 cm air gap the calculated onset voltage is 4.25 kV, while it was measured as 3.91 kV. When the point–plane distance was reduced to

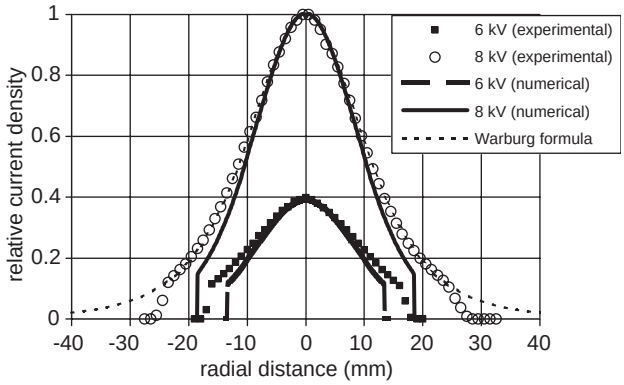

Fig. 6. Experimental versus computational current density distribution on the ground plate for 95 μm tip and 2 cm air gap.

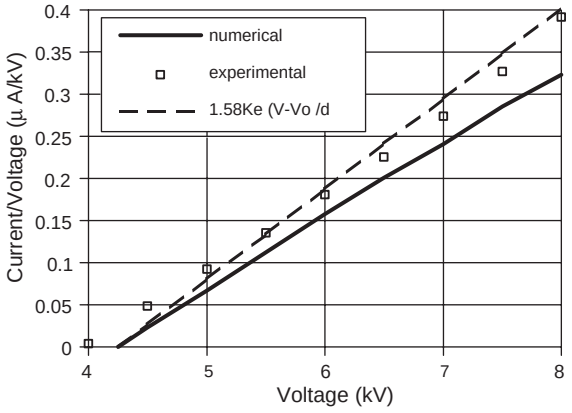

Fig. 7. V/I versus voltage curves for sharp point electrode (35 μm radius of curvature) at 3.1 cm point–plane distance.

2 cm the experimental and computational values are 3.46 kV and 4.06 kV, respectively. While the general trend in I/V versus V curves is still the same, the differences between curves are much larger (Fig. 7).

The experimental curves for the current density agree rather well with the Warburg predictions, except for the points close to the axis at high voltage (Fig. 8). Quite sharp increase of the current density at these points at 7 kV can be probably explained by the presence of streamers and was not observed at the voltage reduced to 5 kV. Computational results yield not only faster decrease of the current density, but also a clearly narrower beam of current. The field gradient for sharp electrodes is very strong and the discretization is not sufficient to model this.

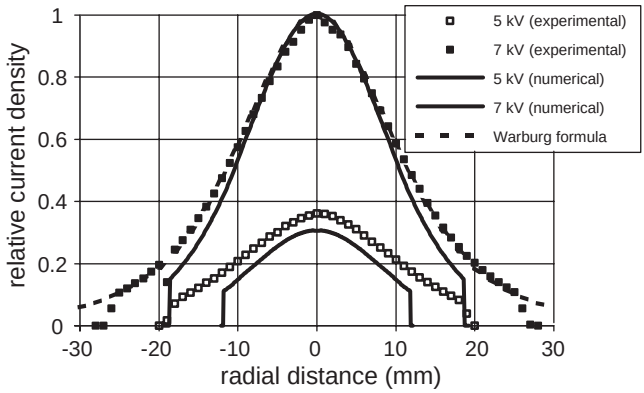

Fig. 8. Computational and experimental current density distributions on the ground plane for a sharp electrode (35 μm) and short point–plane distance (2 cm).

5. Conclusions

The results of the numerical simulation of the electric corona discharge have been compared with the experimental data for the point–plane geometry. Assuming that the mobility of the positive ions is equal to 2.3×10^{-4}, the numerical algorithm predicts reasonably well $V-I$ characteristics of the discharge. The I/V versus V curve is almost perfectly linear and follows a simple analytical formula, with the proportionality coefficient equal to 1.58.

Prediction of the current density distribution on the ground plate is satisfactory if the electrode is not too sharp (radius of curvature equal to 95 μm). For sharper electrodes (35 μm) the accuracy of these calculations is worse, probably due to the inability to correctly simulate a very large field gradient near the electrode tip.

Radius of the non-zero current zone on the ground plate can differ substantially between experiments and simulation. Perhaps, the simple monopolar corona model is not sufficient to predict this parameter accurately.

Acknowledgements

This work was supported in part by Joseph Fourier University and CNRS (through invitation of K. Adamiak to the LEMD) and the Natural Sciences and Engineering Research Council (NSERC) of Canada.

References

[1] R. Morrow, The theory of positive glow corona, J. Phys. D: Appl. Phys. 30 (1997) 3099–3114.
[2] R. Morrow, Theory of negative corona in oxygen, Phys. Rev. A 32 (1985) 1799–1809.

[3] F. Pontiga, C. Soria, A. Castellanos, J.D. Skalny, Physico-chemical modeling of negative corona in oxygen: the effect of boundaries, 2002 Annual Report Conference on Electrical Insulation and Dielectric Phenomena, Cancun, Mexico, October 2002, pp. 797–800.
[4] P. Atten, K. Adamiak, V. Atrazhev, Electric corona discharge simulation in the hyperbolic point—ground plane configuration, 2002 Annual Report Conference on Electrical Insulation and Dielectric Phenomena, Cancun, Mexico, October 2002, pp. 109–112.
[5] J.Q. Feng, Application of Galerkin finite-element method with Newtonian iterations in computing steady-state solutions of unipolar charge current in corona devices, J. Comput. Phys. 151 (1999) 969–989.
[6] J.R. McDonald, W.B. Smith, H.W. Spencer III, L.E. Sparks, A mathematical model for calculating electrical conditions in wire–duct electrostatic precipitation devices, J. Appl. Phys. 48 (1977) 2231–2243.
[7] S. Cristina, G. Dinelli, M. Feliziani, Numerical computation of corona space charge and $V-I$ characteristics in DC electrostatic precipitators, IEEE Trans. Ind. Appl. 27 (1991) 147–153.
[8] K. Adamiak, Simulation of corona in wire-duct electrostatic precipitator by means of the boundary element method, IEEE Trans. Ind. Appl. 30 (1994) 381–386.
[9] J.L. Davies, J.F. Hoburg, Wire–duct precipitator field and charge computation using finite element and characteristics methods, J. Electrostat. 14 (1983) 187–199.
[10] P.L. Levin, J.F. Hoburg, Donor cell—finite elements descriptions of wire–duct precipitator fields, charges and efficiencies, IEEE Trans. Ind. Appl. 26 (1990) 662–670.
[11] M. Abdel-Salam, Z. Al-Hamouz, Finite-element analysis of monopolar ionized fields including ion diffusion, J. Phys. D: Appl. Phys. 26 (1993) 2202–2211.
[12] K. Adamiak, Particle charging by unipolar ionic bombardment in an AC electric field, IEEE Trans. Ind. Appl. 33 (1997) 421–426.
[13] T.G. Beuthe, J.-S. Chang, Gas discharge phenomena, in: J.-S. Chang, et al., (Eds.), Handbook of Electrostatic Processes, Marcel Dekker, New York, 1995, p. 165.
[14] L.B. Loeb, Fundamental Processes of Electrical Discharge in Gases, Wiley, New York, 1939.
[15] N.A. Kaptzov, Elektricheskiye Yavleniya v Gazakh i Vacuume, OGIZ, Moscow, 1947.
[16] A.M. Meroth, T. Gerber, C.D. Munz, P.L. Levin, A.J. Schwab, Numerical solution of nonstationary charge coupled problems, J. Electrostat. 45 (1999) 177–198.
[17] C.A. Brebbia, J.C.F. Telles, L.C. Wrobel, Boundary Element Techniques, Springer, Berlin, 1984.
[18] M.N.O. Sadiku, Numerical Techniques in Electromagnetics, CRC Press, Boca Raton, 1992.
[19] K. Adamiak, Application of integral equations to solving inverse problems of stationary electromagnetic fields, Int. J. Numer. Meth. Eng. 21 (1985) 1447–1458.
[20] J.M. Crowley, Fundamentals of Applied Electrostatics, Wiley, New York, 1986, pp. 94–97.
[21] K. Adamiak, P. Atten, Simulation de la decharge couronne en configuration pointe-plan, SFE2002—3eme Congress Annuel de la Société Française d'Electrostatique, Toulouse, France, July 3–4, 2002, pp. 1–8.
[22] J.A. Cross, Electrostatics: Principles, Problems and Applications, Adam Hilger, Bristol, 1987, pp. 277.
[23] R.S. Sigmond, Simple approximate treatment of unipolar space-charge-dominated coronas: the Warburg law and the saturation current, J. Appl. Phys. 53 (1982) 891–898.
[24] A. Goldman, M. Goldman, J.E. Jones, M. Yumato, Current distributions on the plane for point-plane negative coronas in air, nitrogen and oxygen, IX International Conference on Gas Discharges and Their Applications, Venezia, Italy, September 19–23, 1988, pp. 197–200.